



# Drought-Induced Carbon and Water Use Efficiency Responses in Dryland Vegetation of Northern China

Chengcheng Gang<sup>1,2,3</sup>, Yi Zhang<sup>2</sup>, Liang Guo<sup>1,2</sup>, Xuerui Gao<sup>1,2</sup>, Shouzhang Peng<sup>1,2</sup>, Mingxun Chen<sup>4</sup> and Zhongming Wen<sup>1,2\*</sup>

<sup>1</sup> Institute of Soil and Water Conservation, Northwest A&F University, Yangling, China, <sup>2</sup> Institute of Soil and Water Conservation, Chinese Academy of Sciences and Ministry of Water Resources, Yangling, China, <sup>3</sup> International Center for Climate and Global Change Research, School of Forestry and Wildlife Sciences, Auburn University, Auburn, AL, United States, <sup>4</sup> College of Agronomy, Northwest A&F University, Yangling, China

## OPEN ACCESS

### Edited by:

Zhiyou Yuan,  
College of Forestry, Northwest A&F  
University, China

### Reviewed by:

Zhaoqi Wang,  
Peking University, China  
Jinsong Wang,  
Institute of Geographic Sciences  
and Natural Resources Research  
(CAS), China  
Wen Yang,  
Shaanxi Normal University, China

### \*Correspondence:

Zhongming Wen  
zmwen@ms.iswc.ac.cn

### Specialty section:

This article was submitted to  
Plant Abiotic Stress,  
a section of the journal  
Frontiers in Plant Science

**Received:** 15 October 2018

**Accepted:** 11 February 2019

**Published:** 26 February 2019

### Citation:

Gang C, Zhang Y, Guo L, Gao X,  
Peng S, Chen M and Wen Z (2019)  
Drought-Induced Carbon and Water  
Use Efficiency Responses in Dryland  
Vegetation of Northern China.  
*Front. Plant Sci.* 10:224.  
doi: 10.3389/fpls.2019.00224

Given the context of global warming and the increasing frequency of extreme climate events, concerns have been raised by scientists, government, and the public regarding drought occurrence and its impacts, particularly in arid and semi-arid regions. In this paper, the drought conditions for the forest and grassland areas in the northern region of China were identified based on 12 years of satellite-based Drought Severity Index (DSI) data. The impact of drought on dryland vegetation in terms of carbon use efficiency (CUE) and water use efficiency (WUE) were also investigated by exploring their correlations with DSI. Results indicated that 49.90% of forest and grassland experienced a dry trend over this period. The most severe drought occurred in 2001. In general, most forests in the study regions experienced near normal and wet conditions during the 12 year period. However, grasslands experienced a widespread drought after 2006. The forest CUE values showed a fluctuation increase from 2000 to 2011, whereas the grassland CUE remained steady over this period. In contrast, WUE increased in both forest and grassland areas due to the increasing net primary productivity (NPP) and descending evapotranspiration (ET). The CUE and WUE values of forest areas were more sensitive to droughts when compared to the values for grassland areas. The correlation analysis demonstrated that areas of DSI that showed significant correlations with CUE and WUE were 17.24 and 10.37% of the vegetated areas, respectively. Overall, the carbon and water use of dryland forests was more affected by drought than that of dryland grasslands.

**Keywords:** carbon use efficiency, drought severity index, dryland vegetation, northern China, water use efficiency

## INTRODUCTION

Recently, droughts have been frequently recorded due to climatic warming from elevated concentrations of greenhouse gasses. This warming exacerbates water resource stress and poses a significant threat to food security and the sustainability of human activities in these areas (Vorosmarty et al., 2000; Rosegrant et al., 2003). The reports of the Intergovernmental Panel on Climate Change suggest that drought frequency will likely increase by the end of 21st century, particularly in regions that are currently dry (IPCC, 2014). At the ecosystem scale, drought

will reduce the carbon sequestration ability of vegetation and aggravate the water evaporation rate of ecosystems (Ciais et al., 2005; Zhao and Running, 2010). The ecosystem-scale carbon use efficiency (eCUE), which is defined as the ratio of net primary productivity (NPP) to gross primary productivity (GPP), describes the capacity of an ecosystem to transfer the carbon from the atmosphere to vegetation biomass (DeLucia et al., 2007). The ecosystem-scale water use efficiency (eWUE), a ratio of NPP to evapotranspiration (ET), measures the net carbon uptake per amount of water lost from the ecosystem (Beer et al., 2009; Gang et al., 2016a,b). The eCUE and eWUE are two vital indicators for addressing the ecosystem function in terms of carbon and water cycles (Webb et al., 1978; LeHouerou, 1984; DeLucia et al., 2007). The satellite-based imageries provide an effective way in monitoring drought severity and vegetation responses in term of carbon and water cycles (AghaKouchak et al., 2015; Liu Y. et al., 2015). The impacts of droughts on CUE and WUE have been widely reported in multiple scales (Webb et al., 1978; DeLucia et al., 2007; Liu Y. et al., 2015; Gang et al., 2016a). However, the occurrence of drought and its subsequent influences on ecosystem-scale CUE and WUE have not been extensively investigated, especially in the arid and semi-arid regions. Therefore, further research is needed on the extent and duration of droughts as well as their impacts on the carbon and water cycles of dryland vegetation.

Precipitation is a primary input data in most drought indices, which have been widely used in monitoring drought conditions at different levels, such as the Standardized Precipitation Index (SPI) (McKee et al., 1995), the Palmer Drought Severity Index (PDSI) (Palmer, 1965), the Temperature-Vegetation Dryness Index (TVDI) (Sandholt et al., 2002), the Vegetation, Water and Thermal Stress Index (VWTCI) (Shakya and Yamaguchi, 2010), and the Percentage of Precipitation Anomaly (PPA). The large-scale effects of drought on vegetation are detectable with the help of remote sensing technology, which avoids the deficiencies of field-based meteorological observation (Rhee et al., 2010; Rojas et al., 2011). The Normalized Difference Vegetation Index (NDVI), which can reflect the growth status of plants, has been widely used for evaluating the effects of drought on vegetation growth (Cunha et al., 2015; Klisch and Atzberger, 2016). Many NDVI-based drought indicators have also been developed, such as the Anomaly Vegetation Index (AVI) (Chen et al., 1994), the Temperature Vegetation Drought Index (TVDI) (Sandholt et al., 2002), and the Standardized Vegetation Index (SVI) (Peters et al., 2002). ET, an important component of terrestrial water cycles, is a more direct and effective indicator for reflecting ecosystem moisture status (Mu et al., 2007a, 2011). Remote sensing technology can provide spatially explicit ET information for terrestrial ecosystems (Jackson et al., 2005). Combining the MODIS-derived NDVI and evapotranspiration/potential evapotranspiration (ET/PET) data, Mu et al. (2013) developed a satellite-based drought index with fine resolution at the global scale. This index is known as Drought Severity Index (DSI). The DSI dataset has been proven to be capable of monitoring droughts over the last decade worldwide (Zhao and Running, 2011; Mu et al., 2013; Zhang and Yamaguchi, 2014).

The northwest regions of China and Inner Mongolia (NWIM), which are mainly situated in the northern inland of China, are characterized with a dry climate, scarce precipitation, intensive evaporation, and a fragile environment (Gou et al., 2015). The unique location and climate make these regions vulnerable to climate change and human disturbance. Previous research has demonstrated that Ningxia, Gansu, and Xinjing provinces have experienced different drought conditions in the past decade, and these conditions exerted great influence on environment and agricultural production (Gou et al., 2015; Huang et al., 2015; Wang et al., 2015; Zhang et al., 2016). However, most of these studies mainly focused on the regional scale. The extent and severity of drought occurrences as well as the effects of droughts on carbon and water cycles at the ecosystem scale are still open questions that require further study.

The first decade of the 21st century has been estimated as the warmest period since the 1880s. These extreme temperatures highlight the importance of identifying the drought condition for the dryland vegetation during this particular period (Zhao and Running, 2010). The primary objectives of this study are: (i) to examine the extent and duration of drought events in the forests and grasslands of the NWIM from 2000 to 2011 via remotely sensed DSI data; (ii) to quantify the annual changes of ecosystem-scale CUE and WUE for forests and grasslands during this period; and (iii) to explore the correlations between vegetation CUE, WUE, and climate variables to reveal the environment drivers of vegetation carbon and water utilization. The outcomes of this study will elucidate the extent and duration of drought occurrence in the forests and grasslands of the NWIM region, and the results provide guidance for the initiation of adaptation strategies to respond to the climate extremes.

## MATERIALS AND METHODS

### Study Area

The NWIM region covers three provinces (Shaanxi, Gansu, and Qinghai) and three autonomous regions (Ningxia Hui Autonomous Region, Inner Mongolia Autonomous Region, and Xinjiang Uygur Autonomous Region) between the latitudes of 37–53°N and the longitudes of 73–126°E (Figure 1). The total area of NWIM is approximately  $4.15 \times 10^6$  km<sup>2</sup>, occupying approximately 45% of the land area of China and supporting 10% of the population. Most of this region is characterized by arid and semi-arid climates with mean annual temperatures (MAT) ranging from –7 to 16°C. The mean annual precipitation (MAP) ranges from 10 to 1100 mm (Shi et al., 2007; Mu et al., 2013; Wang H. et al., 2013). The MAP exhibits an obvious latitudinal distribution. Xinjiang and northern Inner Mongolia exhibit lower values and the southern areas of Shaanxi, Gansu, and Qinghai present higher MAP values (Shi et al., 2007).

### Land Use and Land Cover Data

The land use and land cover map of the NWIM region was derived from the International Geosphere-Biosphere Project (IGBP) land cover dataset, which contains 17 land cover classes (Loveland et al., 2000). In this study, closed

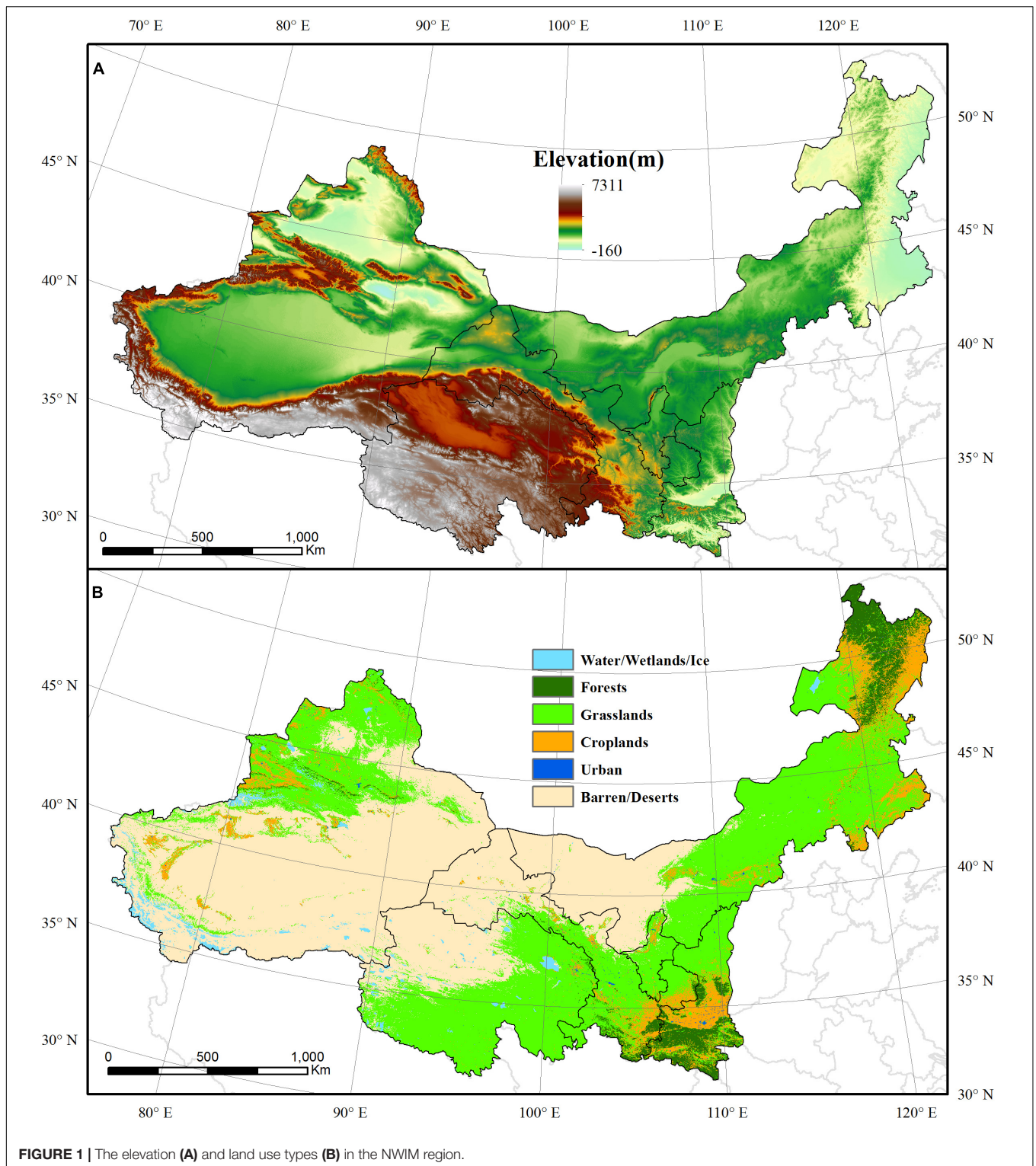


**FIGURE 1 |** The elevation (A) and land use types (B) in the NWIM region.

shrublands, open shrublands, woody savannas, savannas, and non-woody grasslands were regrouped as grasslands. The NWIM region has the largest typical steppe grassland in China, covering more than 41.00% of the total region. Evergreen needle forest, evergreen broadleaf forest, deciduous

needle forest, and mixed forests were reclassified as forests, and these areas account for 4.70% of the total NWIM region. Barren/deserts, occupying 44.80% of the region, is the mostly widely distributed land use type in the NWIM region. Water bodies, croplands, and urban area made

up to 1.52, 7.69, and 0.24% of total area, respectively. Only the grassland and forest areas were included in the following analyses.

## MODIS DSI, GPP, NPP, and ET Data

The annual MODIS DSI, GPP, NPP, and ET data from 2000 to 2011 for the NWIM region were obtained from the Numerical Terra dynamic Simulation Group at the University of Montana<sup>1</sup>. The DSI (0.05° spatial resolution) was based on the basis of ET/PET and snow-free growing season MODIS NDVI products for all vegetated land areas (Atkinson et al., 2011; Mu et al., 2013). The NDVI has been widely used to monitor the global vegetation photosynthetic activities due to its sensitivity to vegetation drought responses and associated water stress, especially in the water-limited regions (Huete et al., 2002; Justice et al., 2002). DSI is calculated as a standardized value, and its equation is expressed as follows:

$$SA_{NDVI} = \frac{NDVI - \overline{NDVI}}{\delta_{NDVI}} \quad (1)$$

$$SA_{EVA} = \frac{(ET/PET) - \overline{(ET/PET)}}{\delta_{(ET/PET)}} \quad (2)$$

$$SA = SA_{NDVI} + SA_{EVA} \quad (3)$$

$$DSI = \frac{SA - \overline{SA}}{\delta_{SA}} \quad (4)$$

where  $SA_{NDVI}$ , the standardized anomaly of the NDVI, is calculated using the long-term mean value of  $\overline{NDVI}$  and the standard deviation  $\delta_{NDVI}$  during the period 2000–2011;  $SA_{EVA}$ , the standardized anomaly of  $ET/PET$ , is calculated as the long-term mean value of  $\overline{ET/PET}$  and a standard deviation  $\delta_{(ET/PET)}$ ;  $ET/PET$  means the ratio of ET to PET;  $SA$  is a sum of  $SA_{NDVI}$  and  $SA_{EVA}$ ; the DSI is a standardized anomaly of  $SA$ ;  $\overline{SA}$  is the long-term mean value of  $SA_{NDVI}$  and  $SA_{(ET/PET)}$ ;  $\delta_{SA}$  is the standardized deviation. The DSI value can be reclassified into 11 categories to indicate different drought conditions, which is shown in **Table 1** (Mu et al., 2013; Zhang and Yamaguchi, 2014).

The new version of MODIS productivity products have been improved by matching the spatial resolution of metrological data to that of MODIS pixel, filling the missing value of FPAR/LAI data due to cloud contamination and malfunction of MODIS sensor, and updating the biome parameter look-up table according to the productivity data from flux tower measurements (Zhao et al., 2005; Gang et al., 2016a). GPP values are calculated as follows:

$$GPP = \varepsilon_{\max} \times 0.45 \times SW_{\text{rad}} \times FPAR \times fVPD \times fT_{\min} \quad (5)$$

where  $\varepsilon_{\max}$  is the maximum light use efficiency under optimal conditions;  $SW_{\text{rad}}$  is the incoming short-wave solar radiation, of which 45% is Photosynthetically Active Radiation (PAR); FPAR is the fraction of PAR absorbed by the plant canopy;  $fVPD$  is

**TABLE 1** | The categories for drought conditions of the global DSI (Mu et al., 2013).

Category	Description	DSI
D5	Extremely drought	< -1.50
D4	Severe drought	-1.49 to -1.20
D3	Moderate drought	-1.99 to -0.9
D2	Mild drought	-0.89 to -0.60
D1	Incipient drought	-0.59 to -0.30
WD	Near normal	-0.29 to 0.29
W1	Incipient wet	0.30 to 0.59
W2	Slightly wet	0.60 to 0.89
W3	Moderately wet	0.90 to 1.19
W4	Very wet	1.20 to 1.50
W5	Extremely wet	> 1.50

vapor pressure deficits scalar, and  $fT_{\min}$  is the daily minimum temperature ( $T_{\min}$ , °C) scalar.

NPP is calculated by subtracting the maintenance and growth respiration from GPP. It is calculated as follows:

$$NPP = \sum_1^{365} GPP - R_{m\_lr} - R_{m\_w} - R_g \quad (6)$$

where  $R_{m\_lr}$  is the maintenance respiration from living leaves and fine roots, and  $R_{m\_w}$  is the annual maintenance respiration from living wood,  $R_g$  is annual growth respiration. Detailed description for modeling MODIS GPP and NPP can be found in Zhao et al. (2005, 2006). Ecosystem-scale CUE for vegetation was calculated as the ratio of annual NPP to GPP in each grid.

The ET represents transpiration by vegetation and evaporation from canopy and soil surfaces. Based on the Penman-Monteith equation, the new version of MODIS ET dataset improved in many aspects, including the recalculation of the fraction of vegetation cover, the soil heat flux, and boundary layer resistance (Mu et al., 2007a,b, 2011). The ET algorithm is computed as follows:

$$\lambda E = \lambda E_{\text{wet\_C}} + \lambda E_{\text{trans}} + \lambda E_{\text{SOIL}} \quad (5)$$

Where  $\lambda E$  is the total daily ET,  $\lambda E_{\text{wet\_C}}$  refers to evaporation from the wet canopy surface,  $\lambda E_{\text{trans}}$  means the transpiration from the dry canopy surface, and  $\lambda E_{\text{SOIL}}$  is the evaporation from the soil surface (Mu et al., 2007a,b, 2011). The MODIS ET product has been validated and widely used in regional and global research (Mu et al., 2011; Gang et al., 2016a). The ecosystem-scale WUE for vegetation was calculated as the ratio of annual NPP to ET in each grid. The MODIS GPP, NPP, and ET performed reliable estimation accuracy on vegetation in northern China (Wang X. et al., 2013; Xiao, 2014; Liu Z. et al., 2015).

## Climate Factor Data

Meteorological data, including temperature and precipitation, from 2000 to 2011 were obtained from the China Meteorological Data Service Center<sup>2</sup>. The monthly data, interpolated by using ANUSPLIN, were used to generate the gridded MAT and MAP.

<sup>1</sup><http://www.ntsug.umt.edu/>

<sup>2</sup><http://data.cma.cn/>

## Analysis of Temporal Dynamic

Equation 6 was used to quantify the linear trend of variables (including DSI, CUE, WUE, NPP, GPP, ET, MAT, and MAP) via the ordinary least square estimation:

$$\text{Slope} = \frac{n \times \sum_{i=1}^n i \times Va_i - \left( \sum_{i=1}^n i \right) \left( \sum_{i=1}^n Va_i \right)}{n \times \sum_{i=1}^n i^2 - \left( \sum_{i=1}^n i \right)^2} \quad (6)$$

where  $i$  starts 1 for the year 2000, 2 for year 2001, and goes up to 12 for 2011; and  $Va_i$  refers to the annual value of variable at time  $i$ ,  $i = 1, \dots, n$ ,  $n = 12$ . The positive value of *Slope* in Eq. (6) indicates an increasing trend of variable, while the negative value connotes a decreasing trend during the 12-year period.

## Correlation Analysis of Climate Variables With Vegetation CUE and WUE

The correlations of vegetation CUE and WUE with climate variables, including DSI, MAP, and MAT, were calculated to reveal the controlling of climate variables that impact CUE and WUE. If the correlation coefficient passes the significance test, then an extremely significant (at 99% confidence level) or significant (at 95% confidence level) linear correlation is indicated.

## RESULTS

### Drought Characteristics of Forest and Grassland in the NWIM Region

During the period of 2000–2011, the area of regions that became increasingly dry accounted for 49.90% of the total area of forest and grassland. These areas were mainly located in eastern Inner Mongolia and northern Xinjiang. The total area of regions that exhibited increasingly wetness was a little larger than the area exhibiting aridity. There regions with increasing wetness were mainly distributed within the 30–40°N, including the northern Shaanxi, Ningxia, Gansu, and Qinghai (Figure 2A). Nearly  $3.73 \times 10^4$  km<sup>2</sup> of the forest regions that were dry in 2000 became wet in 2011. The areas under near normal conditions underwent the most obvious changes. Meanwhile, the forest regions that changed from wet to dry conditions reached an area of  $15.56 \times 10^4$  km<sup>2</sup>. This is far larger than the regions that became wet over the same period (Figure 2B). In contrast,  $86.08 \times 10^4$  km<sup>2</sup> of the dry regions of grassland became wet during the 12-year period. Regions under D3 conditions were the largest contribution to this trend. The wet grassland area that became dry was relatively smaller, with the D2 condition making the largest contribution to such change.

In 2001, 62.66% of forest regions were under dry conditions, and 38.90% were under extremely dry conditions (Figure 3). Meanwhile, 71.61% of grassland regions experienced drought, in which 32.51% were under D4 and D5 conditions. Most of forest and grassland regions were under wet conditions between

2002 and 2005. Both forest and grassland regions experienced an obvious drought in 2006. During 2006, 78.59% of the forest area and 55.49% of the grassland area were under dry conditions. Despite the widespread of dry conditions in 2006, most of regions were under D1–D3 conditions. After 2006, most of the forest regions were in wet conditions except in 2008 and 2011. Different drought levels occurred in most of the grassland regions until 2010. Overall, regions under wet conditions expanded gradually during the first half of the study period, and the dry spells expanded gradually in the grassland regions thereafter.

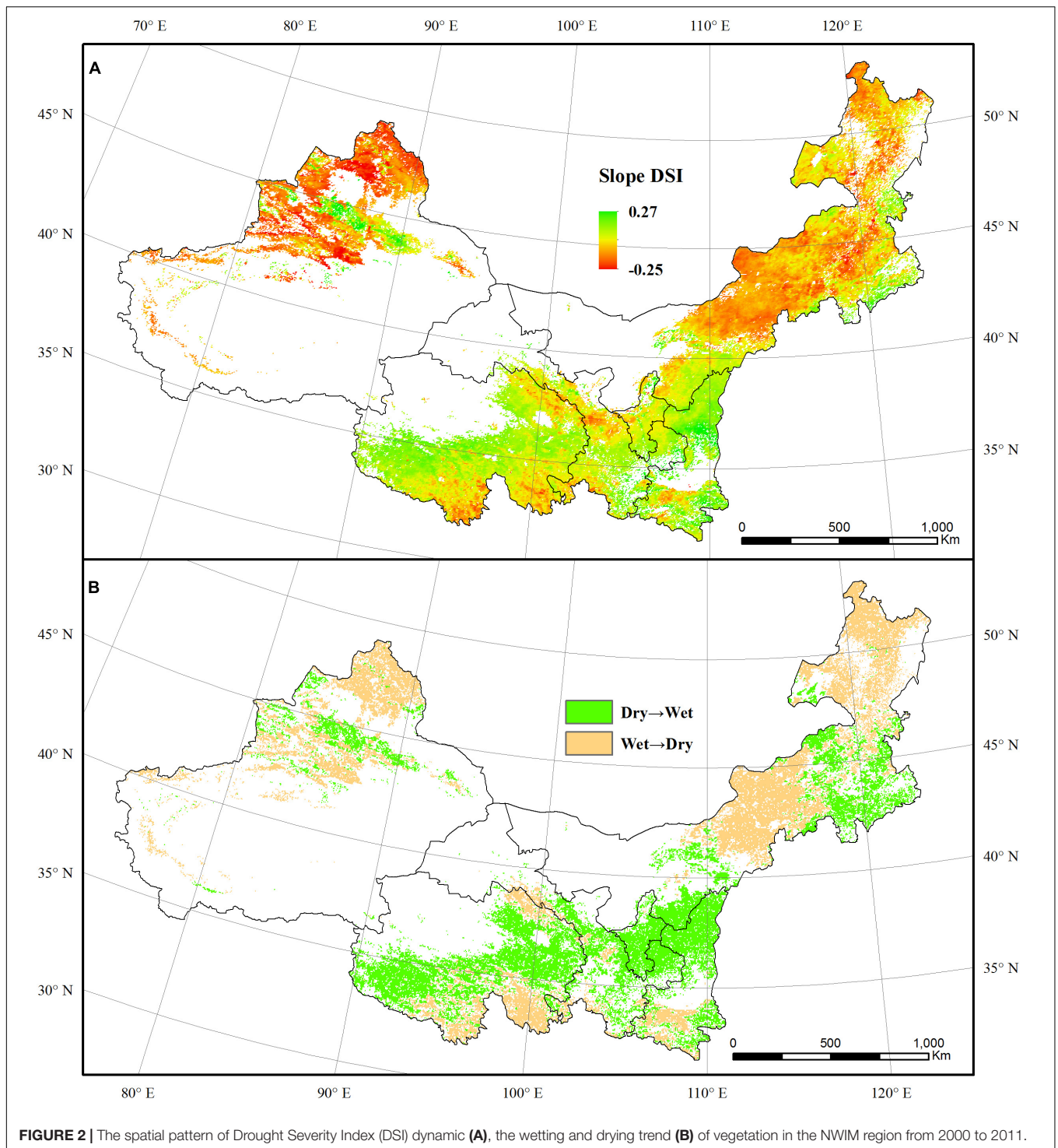
## The Spatiotemporal Dynamics of Vegetation CUE and WUE

The spatial dynamics of CUE and WUE for forest and grassland were firstly evaluated. 53.74% of forest and grassland regions showed an overall increasing trend of CUE over the entire study period, which mainly distributed in eastern Mongolia, and southern Shaanxi. Regions showing decreased CUE mainly occurred in the mid-west of Inner Mongolia, northern Shaanxi, and Tianshan Mountains region. In contrast, WUE increased in 85.98% of forest and grassland regions. Regions showing a decreased WUE mainly distributed in southern Gansu and northwestern Qinghai (Figure 4).

The annual CUE, WUE, and DSI during this period were plotted against time. The average CUE of grassland during the 12-year period was 0.60, higher than that of forest (0.41) for the same period (Figure 5). The value of grassland CUE remained steady over the past 12 years. WUE of forest exhibited fluctuating increase from 2000 to 2011, and the minimum and maximum values exhibited in 2001 and 2009, respectively. The range of change for grassland WUE was less drastic than that for forest. The WUE of grassland also peaked in 2009. The overall variation in forest and grassland DSI can be divided into three stages: the wetting trend from 2000 to 2004, the drying trend from 2004 to 2009, and the wet recovery from 2009 to 2011. The most severe drought occurred in 2001. Averagely, the forest and grassland experienced wet conditions in 3 years, while drought occurred in forest and grassland areas in 2001, 2006, and 2008. In all other years, forest and grassland regions were under near normal conditions. The spatiotemporal dynamics of GPP, NPP, and ET were presented in the **Supplementary Material**.

## The Controlling of Climatic Variables on Vegetation CUE and WUE

The correlations of vegetation CUE and WUE with DSI, MAP, and MAT were calculated to reveal the sensitivity of the vegetation carbon and water use to drought and climate variables. Regions with significant correlations (at 95 and 99% confidence level) between CUE and DSI amounted to 17.24% of the total study area. Area of forest regions that showed significant correlations (at 95 and 99% confidence level) between CUE and DSI reached 29.68% of the total forest regions, and 28.96% of this area exhibited positive correlations. For grassland, regions presenting significant positive and negative correlations between CUE and DSI accounted



for 5.23 and 3.04% of total grassland area, respectively. Regions showing significant correlations (at 95 and 99% confidence level) between CUE and MAP accounted for 10.52% of the total area. These regions were mainly located in eastern Inner Mongolia, southern Shaanxi, and Qinghai (**Figure 6**). For forest, 15.20% of the area showed significant correlations between CUE and MAP, with 11.09% exhibiting

positive correlations and 4.11% exhibiting negative correlation. In contrast, 17.47% of grassland regions showed significant correlations (at 95 and 99% confidence level) between CUE and MAP, in which 7.85% were positive correlations and 9.62% were negatively correlations. There were significant correlations between CUE and MAT in 7.79% of forest regions and 9.92% of grassland regions (at 95 and 99% confidence level), respectively.

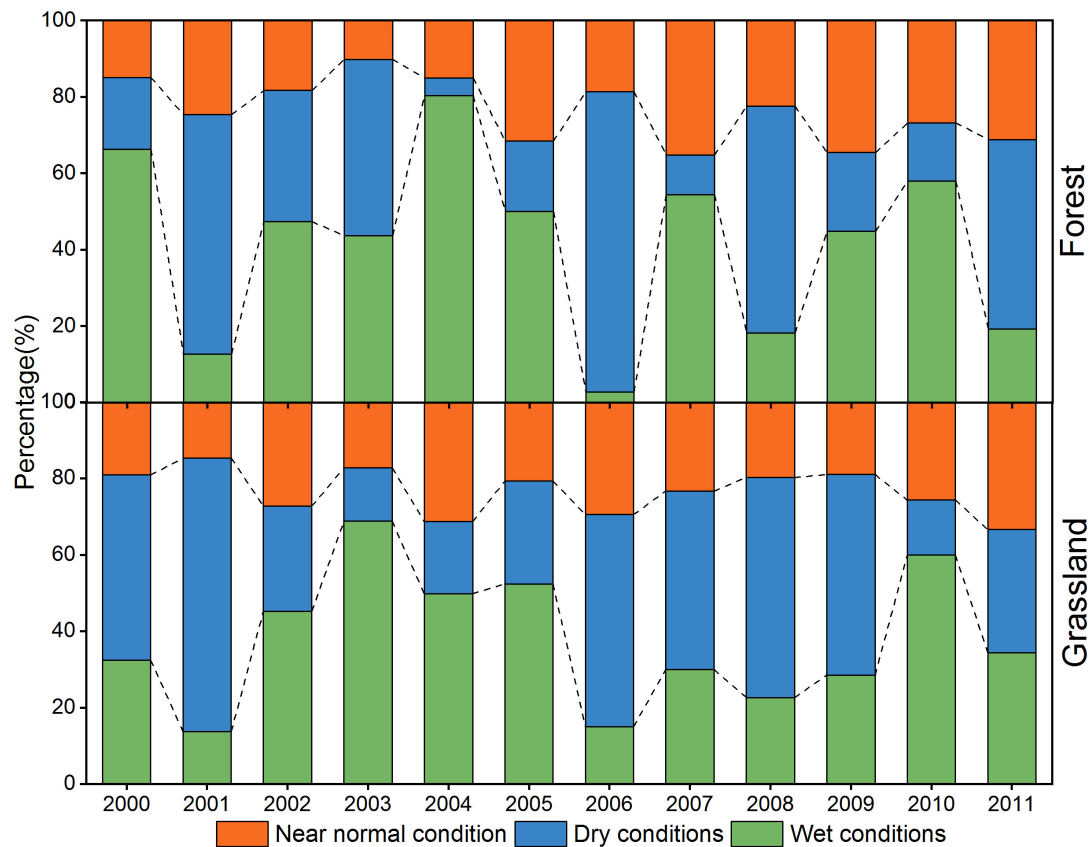


**FIGURE 3** | The percentage change of dry, wet, near normal conditions for forest and grassland during 2000–2011.

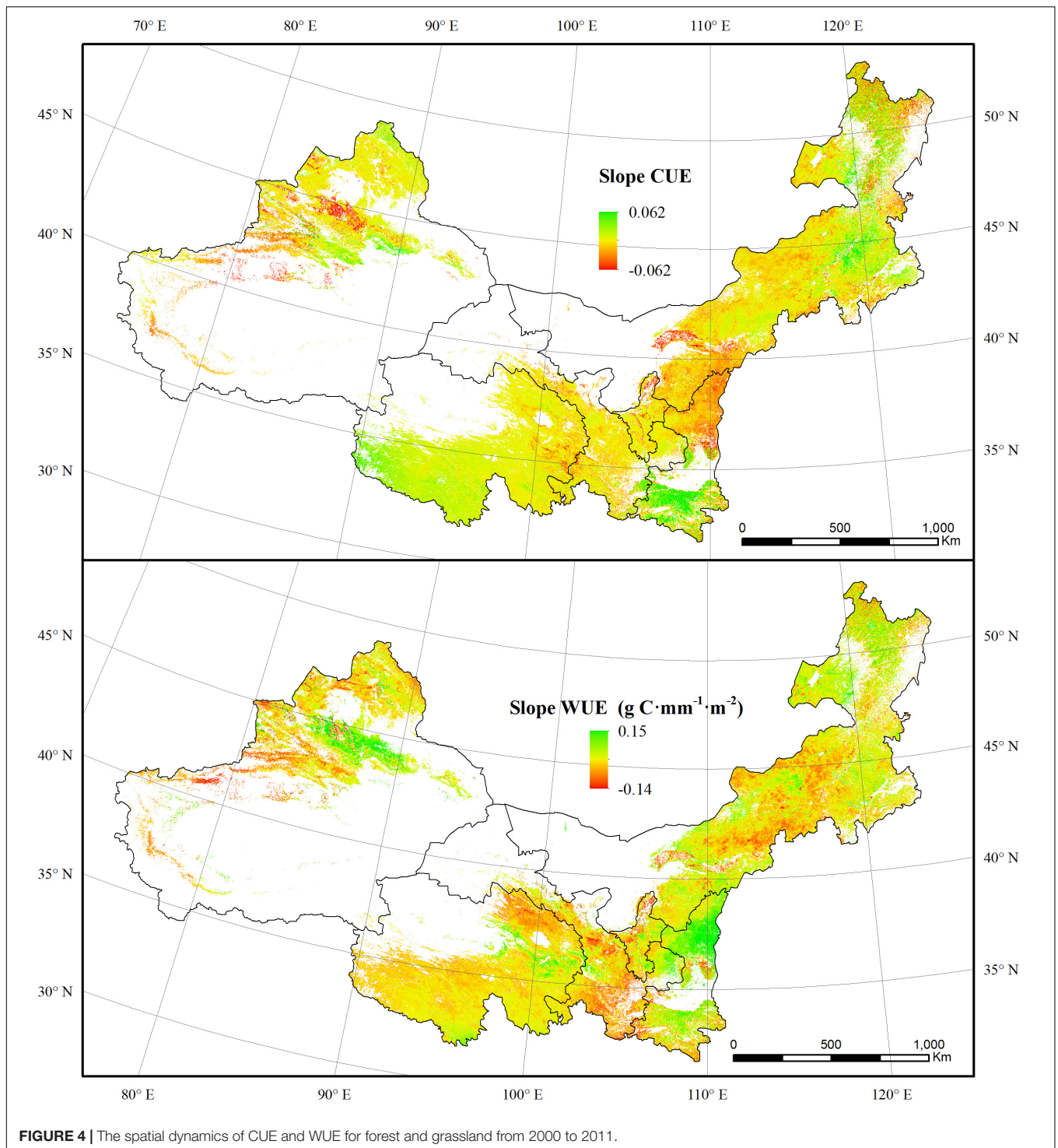
Grassland regions showing significant positive and negative correlations (at 95 and 99% confidence level) between CUE and MAT accounted for 5.99 and 3.94% of total grassland areas, respectively.

Regions with significant correlations (at 95 and 99% confidence level) between WUE and DSI, MAP, and MAT accounted for 10.37, 12.48, and 8.67% of the total study area, respectively. These regions were mainly located in eastern Inner Mongolia, Ningxia, and southern Qinghai (Figure 7). Regions that showed a significant correlation (at 95 and 99% confidence level) between WUE and DSI accounted for 15.89% of the forest area and 9.70% of the grassland area. The forest area with significant positive correlations (at 95 and 99% confidence level) between WUE and DSI was larger than the area with significant negative correlations (11.33% vs. 4.56%). Forest WUE was more correlated with MAP. Regions with significant correlations (at 95 and 99% confidence level) between WUE and MAP amounted to 35.68% of the total forest area, and 34.17% of these regions exhibited positive correlation. Forest WUE exhibited significant negative correlation (at 95 and 99% confidence level) with MAT over 4.23% of the forest area, and 1.02% of the forest region exhibited significant positive correlation. For grassland, regions showing significant positive correlations (at 95 and 99% confidence level) between WUE and DSI, MAP, and MAT were larger

than those showing the negative correlations. WUE exhibited positive correlations with DSI, MAP, and MAT in 5.91, 5.53, and 7.58% of total grassland area, respectively, and showed negative correlations in 3.78, 4.13 and 1.52% of total grassland area, respectively.

## DISCUSSION

In this study, the drought status and its impacts on dryland vegetation in northern China was evaluated by exploring the satellite-based data. Drought severity in forest and grassland as well as its influence on CUE and WUE at the ecosystem scale were investigated. During the period of 2000–2011, most of the forest and grassland in the NWIM region were in near normal and wet conditions. The widespread droughts mainly occurred in 2001 and 2006, and the drought in 2001 was the most severe across the entire study period. Previous studies have demonstrated that widespread and large droughts were frequently recorded in northern China since the late 1990s, and they intensified after 2000. The 2001 drought is considered to be one of the most severe droughts in terms of distribution and duration, which led to extensive agricultural and economical losses (Zhang et al., 2016). The strength of the East Asian summer monsoon in the developing and decaying



phases of El Niño and La Niña events is probably one of the reasons that precipitated the recent drought in northern China (Yu et al., 2014).

Drought affects the vegetation carbon and water utilization mainly through influencing the photosynthesis and ET processes, particularly in regions where water supply is limited (Gang et al., 2016a). In this study, both the NPP and GPP

for grassland increased during the 2000–2011 period. This synchronic changing pattern led to a steady state of grassland CUE during this period. In contrast, forest CUE was more sensitive to drought. The forest CUE presented a weak increasing trend with a curve similar to that of NPP. This was probably caused by the different sensitivities of forest NPP and GPP to the drought conditions (Zhang et al., 2014). In contrast,

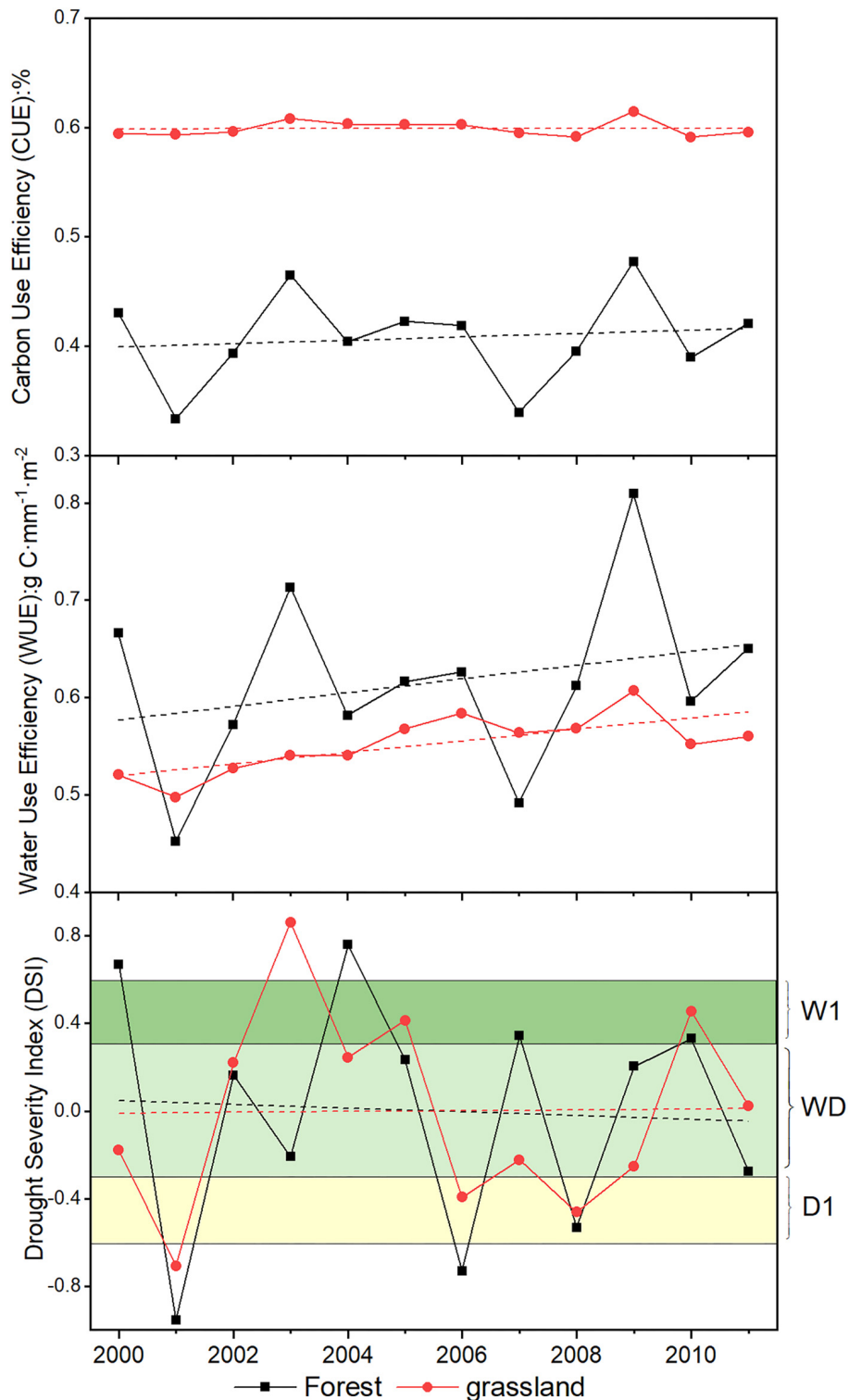


**FIGURE 5 |** The temporal dynamics of CUE, WUE, and DSI for forest and grassland from 2000 to 2011.

the rising NPP and decreasing ET both contributed to the overall ascending trend of WUE for forest and grassland. The WUE increased obviously in the Tianshan Mountains region

and northern Shaanxi (Figure 4). The revegetation due to the “Grain for Green” project in the Loess Plateau has significantly increased the vegetation NPP during the past several decades

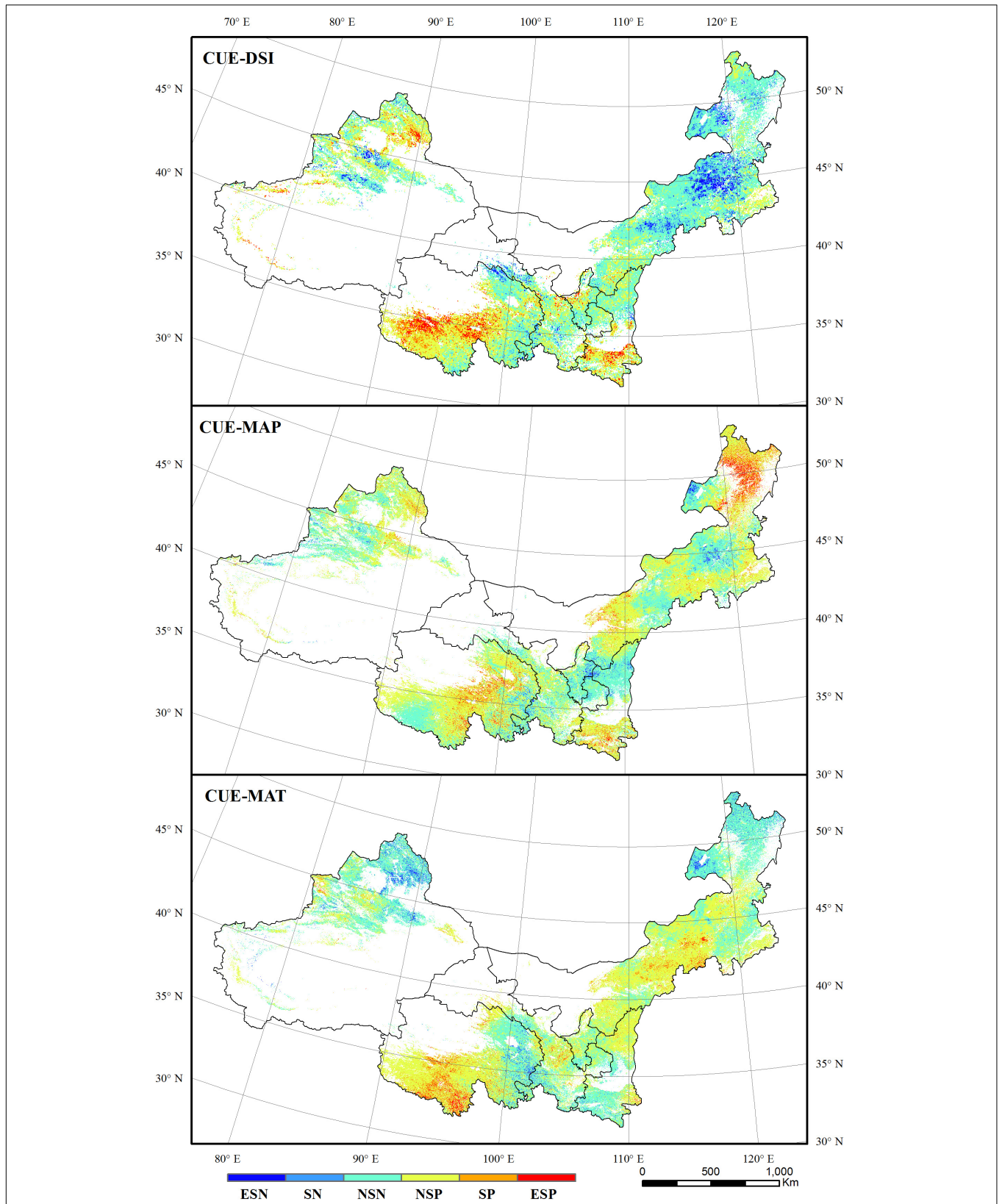


**FIGURE 6 |** The correlations between grassland CUE and DSI, MAP, and MAT. ESN, extremely significant negative; SN, significant negative; NSN, non-significant negative; NSP, non-significant positive; SP, significant positive; ESP, extremely significant positive.

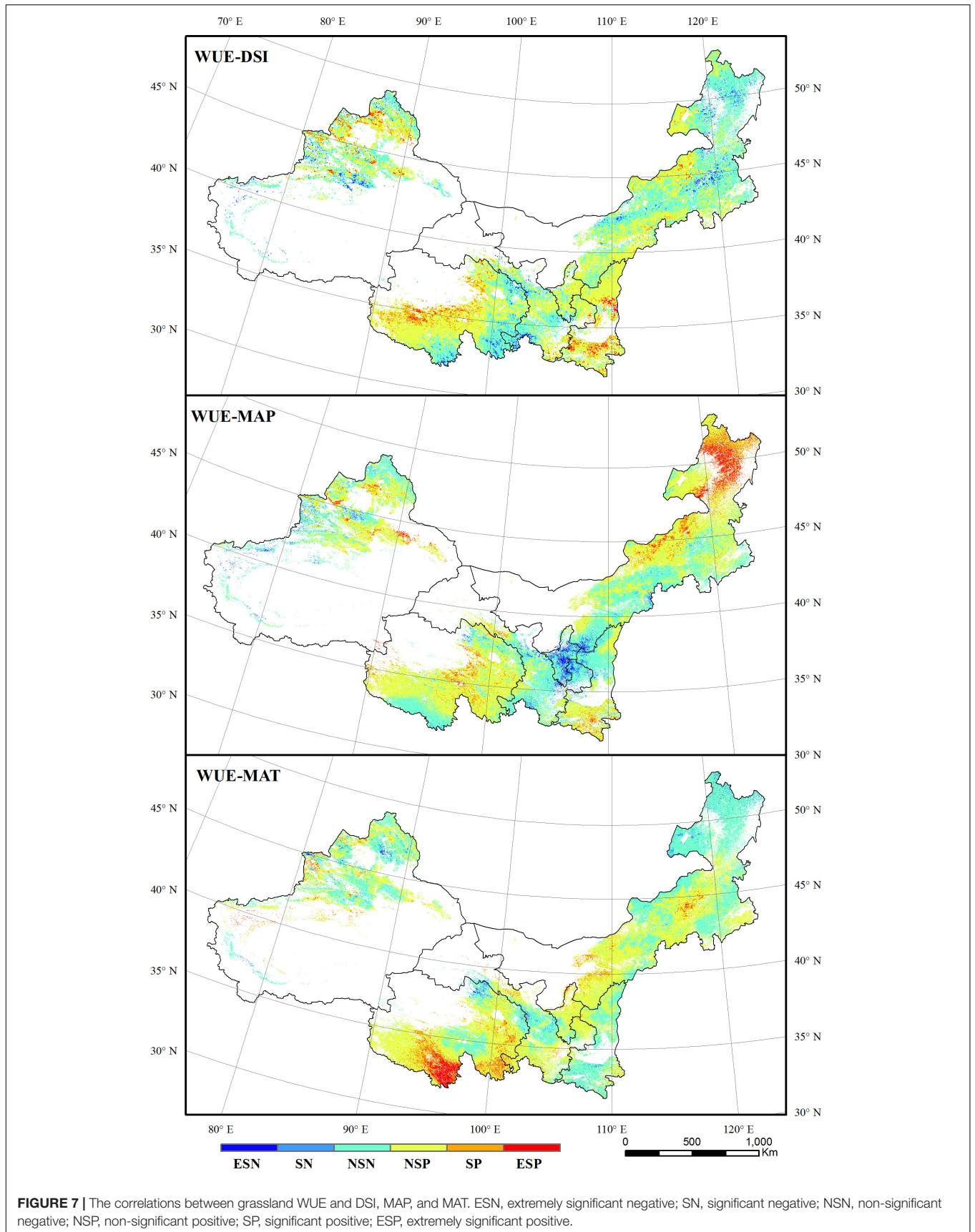
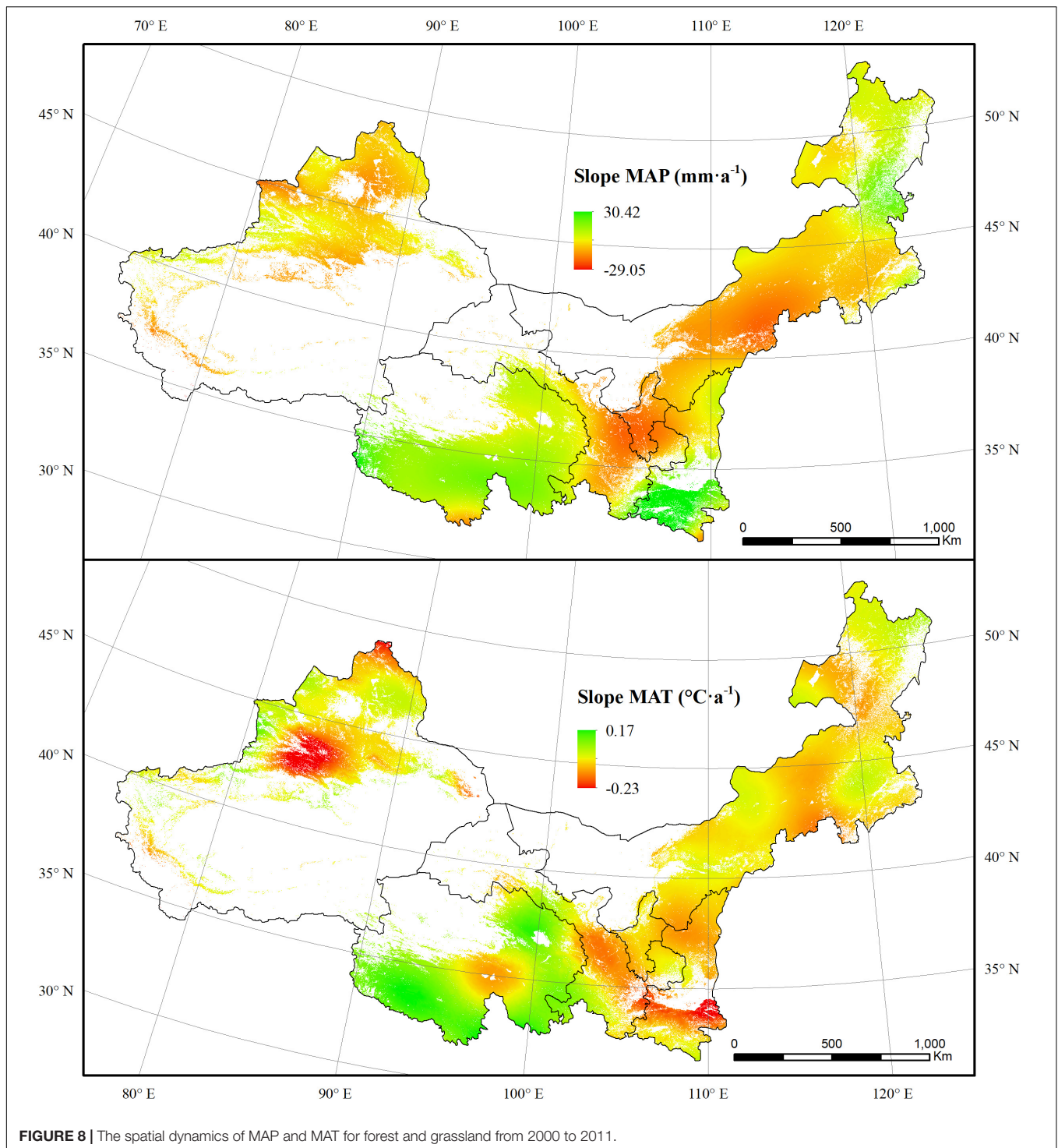


**FIGURE 7 |** The correlations between grassland WUE and DSI, MAP, and MAT. ESN, extremely significant negative; SN, significant negative; NSN, non-significant negative; NSP, non-significant positive; SP, significant positive; ESP, extremely significant positive.



(Xiao, 2014; Deng et al., 2017). The Tianshan Mountains region experienced a cooling trend, which probably is the leading reason for the WUE increase (Figure 8) (Guan et al., 2015). The canopy transpiration, net photosynthesis, and CO<sub>2</sub> exchange were constrained by soil moisture (Mu et al., 2013). Soil moisture status affects the responses of heterotrophic respiration and photosynthesis to temperature. When experiencing a slight

drought, the net photosynthesis rate of plants would decrease due to the reduced activity of ribulose diphosphate carboxylase and reduced photosynthetic capacity of mesophyll cells (Zhou et al., 2009). The widespread drought that occurred in 2006 did not lead to sudden drops in CUE and WUE values in 2006. However, there were drops in 2007. This indicates that the effects of drought might accumulate and appear in the

following years. However, the photosynthetic organs of plants would be damaged under severe drought conditions. This would reduce plant water loss and photosynthesis (Arneeth et al., 1998; Tian et al., 2009). This effect explains the obvious decreases of CUE and WUE in the 2001, when a widespread severe drought was recorded.

The correlation between vegetation WUE and DSI was relatively lower than the correlation between CUE and DSI. This implies that WUE was less sensitive to droughts than CUE for dryland vegetation in northern China. Drought affects the vegetation CUE mainly via the photosynthesis process (Gang et al., 2016b). Regions in eastern Inner Mongolia that are primarily vegetated by meadow showed significant negative correlations between CUE and DSI. The CUE increased in these regions despite a drying trend that was observed during 2000–2011. This increasing trend of CUE was probably caused by human interference, such as fencing or irrigation (Zhang et al., 2015; Yan et al., 2018). Regions showing significant positive correlations between CUE and DSI were mainly located in the northern fringe of Qinghai where became wet during the 12 years. The rising precipitation promotes the increase of both NPP and GPP in these regions (Bai et al., 2013). WUE can be affected by both the photosynthesis and ET process (Tian et al., 2010). Under slight and moderate drought conditions, the vegetation WUE would increase to mitigate the negative effects of water loss to some extent. This study found that area with significant positive correlations between WUE with MAP was larger than the area exhibiting significant positive correlations between WUE and DSI. This implies that rainfall more directly affected the vegetation WUE. Regions presenting the significant positive correlations between WUE and MAP were mainly distributed in eastern Inner Mongolia, Greater Khingan regions, where coniferous forests were mostly vegetated. Trees, such as *Larix gmelinii*, *Pinus tabulaeformis*, and *Abiescephalonica*, have higher WUE values because of low photosynthesis rates, ET rates, and stomatal conductance values (Lefi et al., 2004; Otieno et al., 2005). The photosynthesis ability can be maintained at a certain level even when a severe drought occurred (Maroco et al., 2000; Ogaya and Peñuelas, 2003; Lefi et al., 2004). Regions with a significant positive correlation between WUE and MAT were mainly distributed in the Three Rivers Source regions. This region is primarily characterized by alpine meadow. Temperature is reported as the primary factor affecting the growth of plants in this region (Xu et al., 2011; Guo et al., 2016).

## CONCLUSION

The dryland vegetation in northern China was deeply influenced by the drought during the 2000–2011 period, and forest and grassland reacted differently to drought conditions. Nearly half of the NWIM region became dry in 2000–2011. The areas of forest that experienced a drying trend was more than four times larger than the areas that became wet, whereas the area of grassland regions presenting a drying trend was closer to the

area showing a wetting trend. The most widespread droughts occurred in 2001 and 2006, and the drought severity was higher in 2001 than 2006. In general, most of the vegetation was under wet conditions during the first half of the study period, and grassland subsequently experienced more frequent drought than forest. The forest CUE increased slightly, whereas the CUE of grassland remained steady over the 12-year period. Meanwhile, the decreased ET values of forest and grassland led to the overall increases in WUE values for forest and grassland. The DSI variation adequately explains the temporal dynamics of forest CUE and WUE over this period. In contrast, the CUE and WUE values for grassland were less sensitive to the recent drought conditions. Although there are a few uncertainties, our results suggest that the carbon and water use of forest in northern China suffered more from the recent droughts than that of grassland. Due to the data availability, only the 12 years of DSI and CUE, and WUE data were evaluated in this study. Given the complexity of drought events and the warming climate, it is important to continuously monitor various drought impacts on ecosystem-scale carbon and water use in dryland vegetation under future climate change.

## DATA AVAILABILITY

All datasets generated for this study are included in the manuscript and/or the **Supplementary Files**.

## AUTHOR CONTRIBUTIONS

CG and ZW conceived and designed the research. CG, YZ, and MC collected the data and performed the research. LG, XG, and SP contributed data analysis and validation. CG wrote the manuscript.

## FUNDING

This work was supported by the National Key Research and Development Program of China (Grant No. 2016YFC0501707), the National Natural Science Foundation of China (Grant No. 31602004), the CAS “Light of West China” program (Grant No. XAB2016B05), and the Fundamental Research Funds for the Central Universities (Grant No. 2452017184), the Special Foundation for State Basic Research Program of China (No. 2014YF210100), the Key cultivation project of Chinese Academy of Sciences “The promotion and management of ecosystem functions of restored vegetation in Loess Plateau, China.” We also appreciate the China Meteorological Data Service Center and the NTSG for sharing dataset.

## SUPPLEMENTARY MATERIAL

The Supplementary Material for this article can be found online at: <https://www.frontiersin.org/articles/10.3389/fpls.2019.00224/full#supplementary-material>

## REFERENCES

- AghaKouchak, A., Farahmand, A., Melton, F. S., Teixeira, J., Anderson, M. C., Wardlow, B. D., et al. (2015). Remote sensing of drought: progress, challenges and opportunities. *Rev. Geophys.* 53, 452–480. doi: 10.1002/2014RG000456
- Arnell, A., Kelliher, F. M., McSeveny, T. M., and Byers, J. N. (1998). Net ecosystem productivity, net primary productivity and ecosystem carbon sequestration in a *Pinus radiata* plantation subject to soil water deficit. *Tree Physiol.* 18, 785–793. doi: 10.1093/treephys/18.12.785
- Atkinson, P. M., Dash, J., and Jeganathan, C. (2011). Amazon vegetation greenness as measured by satellite sensors over the last decade. *Geophys. Res. Lett.* 38, 1–6. doi: 10.1029/2011GL049118
- Bai, S., Shi, J., Xiang, D., and Wang, G. (2013). Spatiotemporal pattern change of precipitation in Qinghai in the last 50 years. *J. Arid Land Resour. Environ.* 27, 148–153.
- Beer, C., Ciais, P., Reichstein, M., Baldocchi, D., Law, B. E., Papale, D., et al. (2009). Temporal and among-site variability of inherent water use efficiency at the ecosystem level. *Glob. Biogeochem. Cycles* 23:GB2018. doi: 10.1029/2008GB003233
- Chen, W. Y., Xiao, Q. G., and Sheng, Y. W. (1994). Application of the anomaly vegetation index to monitor heavy drought in 1992. *Remote Sens. Environ. China* 9, 106–112.
- Ciais, P., Reichstein, M., Viovy, N., Granier, A., Ogee, J., Allard, V., et al. (2005). Europe-wide reduction in primary productivity caused by the heat and drought in 2003. *Nature* 437, 529–533. doi: 10.1038/nature03972
- Cunha, A. P. M., Alvares, R. C., Nobre, C. A., and Carvalho, M. A. (2015). Monitoring vegetative drought dynamics in the Brazilian semiarid region. *Agr. For. Meteorol.* 214, 494–505. doi: 10.1016/j.agrformet.2015.09.010
- DeLucia, E. H., Drake, J. E., Thomas, R. B., and Gonzalez-Meler, M. (2007). Forest carbon use efficiency: is respiration a constant fraction of gross primary production? *Glob. Chang. Biol.* 13, 1157–1167. doi: 10.1111/j.1365-2486.2007.01365.x
- Deng, L., Liu, S., Kim, D. G., Peng, C., Sweeney, S., and Shangquan, Z. (2017). Past and future carbon sequestration benefits of China's grain for green program. *Glob. Environ. Chang.* 47, 13–20. doi: 10.1016/j.gloenvcha.2017.09.006
- Gang, C., Wang, Z., Chen, Y., Yang, Y., Li, J., Cheng, J., et al. (2016a). Drought-induced dynamics of carbon and water use efficiency of global grasslands from 2000 to 2011. *Ecol. Indic.* 67, 788–797. doi: 10.1016/j.ecolind.2016.03.049
- Gang, C., Wang, Z., Zhou, W., Chen, Y., Li, J., Chen, J., et al. (2016b). Assessing the spatiotemporal dynamic of global grassland water use efficiency in response to climate change from 2000 to 2013. *J. Agron. Crop Sci.* 202, 343–354. doi: 10.1111/jac.12137
- Gou, X., Gao, L., Deng, Y., Chen, F., Yang, M., and Still, C. (2015). An 850-year tree-ring-based reconstruction of drought history in the western Qilian Mountains of northwestern China. *Int. J. Climatol.* 35, 3308–3319. doi: 10.1002/joc.4208
- Guan, Y., Wang, R., Li, C., Yao, J., Zhang, M., and Zhao, J. (2015). Spatial-temporal characteristics of land surface temperature in Tianshan Mountains area based on MODIS data. *Chin. J. Appl. Ecol.* 26, 681–688.
- Guo, B., Zhou, Y., Zhu, J., Liu, W., Wang, F., Wang, L., et al. (2016). Spatial patterns of ecosystem vulnerability changes during 2001–2011 in the three-river source region of the Qinghai-Tibetan Plateau. *China. J. Arid Land* 8, 23–35. doi: 10.1007/s40333-015-0055-7
- Huang, J., Xue, Y., Sun, S., and Zhang, J. (2015). Spatial and temporal variability of drought during 1960–2012 in inner Mongolia, north China. *Quatern. Int.* 355, 134–144. doi: 10.1016/j.quaint.2014.10.036
- Huete, A., Didan, K., Miura, T., Rodriguez, E. P., Gao, X., and Ferreira, L. G. (2002). Overview of the radiometric and biophysical performance of the MODIS vegetation indices. *Remote Sens. Environ.* 83, 195–213. doi: 10.1016/S0034-4257(02)00096-2
- IPCC (2014). *Climate change 2014: Impacts, Adaptation and Vulnerability. Part A: Global and Sectoral Aspects. Contribution of Working Group II to the Fifth Assessment Report of the IPCC.* Cambridge: Cambridge University Press.
- Jackson, R. B., Jobbágy, E. G., Avissar, R., Roy, S. B., Barrett, D. J., Cook, C. W., et al. (2005). Trading water for carbon with biological carbon sequestration. *Science* 310, 1944–1947. doi: 10.1126/science.1119282
- Justice, C. O., Townshend, J., Vermote, E. F., Masuoka, E., Wolfe, R. E., Saleous, N., et al. (2002). An overview of MODIS land data processing and product status. *Remote Sens. Environ.* 83, 3–15. doi: 10.1016/S0034-4257(02)00084-6
- Klisch, A., and Atzberger, C. (2016). Operational drought monitoring in Kenya using MODIS NDVI time series. *Remote Sens.* 8:267. doi: 10.3390/rs8040267
- Lefi, E., Medrano, H., and Cifre, J. (2004). Water uptake dynamics, photosynthesis and water use efficiency in field-grown *Medicago arborea* and *Medicago citrina* under prolonged Mediterranean drought conditions. *Ann. Appl. Biol.* 144, 299–307. doi: 10.1111/j.1744-7348.2004.tb00345.x
- LeHouérou, H. N. (1984). Rain use efficiency: a unifying concept in arid-land ecology. *J. Arid Environ.* 7, 213–247.
- Liu, Y., Xiao, J., Ju, W., Zhou, Y., Wang, S., and Wu, X. (2015). Water use efficiency of China's terrestrial ecosystems and responses to drought. *Sci. Rep.* 5:13799. doi: 10.1038/srep13799
- Liu, Z., Shao, Q., and Liu, J. (2015). The performances of MODIS-GPP and-ET products in China and their sensitivity to input data (FPAR/LAI). *Remote Sens.* 7, 135–152. doi: 10.3390/rs70100135
- Loveland, T. R., Reed, B. C., Brown, J. F., Ohlen, D. O., Zhu, Z., Yang, L., et al. (2000). Development of a global land cover characteristics database and IGBP DIScover from 1 km AVHRR data. *Int. J. Remote Sens.* 21, 1303–1330. doi: 10.1080/014311600210191
- Maroco, J. P., Pereira, J. S., and Chaves, M. M. (2000). Growth, photosynthesis and water-use efficiency of two C4 Sahelian grasses subjected to water deficits. *J. Arid Environ.* 45, 119–137. doi: 10.1006/jare.2000.0638
- McKee, T. B., Doesken, N. J., and Kleist, J. (1995). “Drought monitoring with multiple time scales,” in *Proceeding of the Ninth Conference on Applied Climatology*, (Boston, MA: American Meteorological Society), 233–236.
- Mu, Q., Heinsch, F. A., Zhao, M., and Running, S. W. (2007a). Development of a global evapotranspiration algorithm based on MODIS and global meteorology data. *Remote Sens. Environ.* 111, 519–536. doi: 10.1016/j.rse.2007.04.015
- Mu, Q., Zhao, M., Heinsch, F. A., Liu, M., Tian, H., and Running, S. W. (2007b). Evaluating water stress controls on primary production in biogeochemical and remote sensing based models. *J. Geophys. Res.* 112:G01012. doi: 10.1029/2006JG000179
- Mu, Q., Zhao, M., Kimball, J. S., McDowell, N. G., and Running, S. W. (2013). A remotely sensed global terrestrial drought severity index. *Bull. Am. Meteorol. Soc.* 94, 83–98. doi: 10.1175/BAMS-D-11-00213.1
- Mu, Q., Zhao, M., and Running, S. W. (2011). Improvements to a MODIS global terrestrial evapotranspiration algorithm. *Remote Sens. Environ.* 115, 1781–1800. doi: 10.1016/j.rse.2011.02.019
- Ogaya, R., and Peñuelas, J. (2003). Comparative field study of *Quercus ilex* and *Phillyrea latifolia*: photosynthetic response to experimental drought conditions. *Environ. Exp. Bot.* 50, 137–148. doi: 10.1016/S0098-8472(03)00019-4
- Otieno, D. O., Schmidt, M., Kinyamario, J. I., and Tenhunen, J. (2005). Responses of *Acacia tortilis* and *Acacia xanthophloea* to seasonal changes in soil water availability in the savanna region of Kenya. *J. Arid Environ.* 62, 377–400. doi: 10.1016/j.jaridenv.2005.01.001
- Palmer, W. C. (1965). *Meteorological Drought*. Washington, DC: Weather Bureau.
- Peters, A. J., Walter-Shea, E. A., Ji, L., Vina, A., Hayes, M., and Svoboda, M. D. (2002). Drought monitoring with NDVI-based standardized vegetation index. *Photogramm. Eng. Remote Sens.* 68, 71–75.
- Rhee, J. Y., Im, J. H., and Carbone, G. J. (2010). Monitoring agricultural drought for arid and humid regions using multi-sensor remote sensing data. *Remote Sens. Environ.* 114, 2875–2887. doi: 10.1016/j.rse.2010.07.005
- Rojas, O., Vrieling, A., and Rembold, F. (2011). Assessing drought probability for agricultural areas in Africa with coarse resolution remote sensing imagery. *Remote Sens. Environ.* 115, 343–352. doi: 10.1016/j.rse.2010.09.006
- Rosegrant, M. W., Cai, X., and Cline, S. A. (2003). Will the world run dry? Global water and food security. *Environ. Sci. Policy Sustain. Dev.* 45, 24–36. doi: 10.1080/00139150309604555
- Sandholt, I., Rasmussen, K., and Andersen, J. (2002). A simple interpretation of the surface temperature/vegetation index space for assessment of surface moisture status. *Remote Sens. Environ.* 79, 213–224. doi: 10.1016/S0034-4257(01)00274-7
- Shakya, N., and Yamaguchi, Y. (2010). Vegetation, water and thermal stress index for study of drought in Nepal and central northeastern India. *Int. J. Remote Sens.* 31, 903–912. doi: 10.1080/01431160902902617
- Shi, Y., Shen, Y., Kang, E., Li, D., Ding, Y., Zhang, G., et al. (2007). Recent and future climate change in northwest China. *Clim. Chang.* 80, 379–393. doi: 10.1007/s10584-006-9121-7
- Tian, H., Chen, G., Liu, M., Zhang, C., Sun, G., Lu, C., et al. (2010). Model estimates of net primary productivity, evapotranspiration, and water use efficiency in the

- terrestrial ecosystems of the southern United States during 1895–2007. *For. Ecol. Manag.* 259, 1311–1327. doi: 10.1016/j.foreco.2009.10.009
- Tian, Y. Q., Gao, Q., Zhang, Z. C., Zhang, Y., and Zhu, K. (2009). The advances in study on plant photosynthesis and soil respiration of alpine grasslands on the Tibetan Plateau. *Ecol. Environ. Sci.* 18, 711–721. doi: 10.1016/j.foreco.2009.10.009
- Vorosmarty, C. J., Green, P., Salisbury, J., and Lammers, R. B. (2000). Global water resources: vulnerability from climate change and population growth. *Science* 289, 284–288. doi: 10.1126/science.289.5477.284
- Wang, H., Chen, Y., and Pan, Y. (2015). Characteristics of drought in the arid region of northwestern China. *Clim. Res.* 62, 99–113. doi: 10.3354/cr01266
- Wang, H., Chen, Y., Xun, S., Lai, D., Fan, Y., and Li, Z. (2013). Changes in daily climate extremes in the arid area of northwestern China. *Theor. Appl. Climatol.* 112, 15–28. doi: 10.1007/s00704-012-0698-7
- Wang, X., Ma, M., Li, X., Song, Y., Tan, J., Huang, G., et al. (2013). Validation of MODIS-GPP product at 10 flux sites in northern China. *Int. J. Remote Sens.* 34, 587–599. doi: 10.1080/01431161.2012.715774
- Webb, W., Szarek, S., Lauenroth, W., Kinerson, R., and Smith, M. (1978). Primary productivity and water-use in native forest, grassland, and desert ecosystems. *Ecology* 59, 1239–1247. doi: 10.2307/1938237
- Xiao, J. (2014). Satellite evidence for significant biophysical consequences of the "Grain for Green" Program on the Loess Plateau in China. *J. Geophys. Res. Biogeosci.* 119, 2261–2275. doi: 10.1002/2014JG002820
- Xu, W., Gu, S., Zhao, X., Xiao, J., Tang, Y., Fang, J., et al. (2011). High positive correlation between soil temperature and NDVI from 1982 to 2006 in alpine meadow of the three-river source region on the qinghai-tibetan plateau. *Int. J. Appl. Earth Obs.* 13, 528–535. doi: 10.1016/j.jag.2011.02.001
- Yan, Y., Wan, Z., Chao, R., Ge, Y., Chen, Y., Gu, R., et al. (2018). A comprehensive appraisal of four kinds of forage under irrigation in Xilingol, Inner Mongolia, China. *Rangel. J.* 40, 171–178. doi: 10.1071/RJ16084
- Yu, M., Li, Q., Hayes, M. J., Svoboda, M. D., and Heim, R. R. (2014). Are droughts becoming more frequent or severe in China based on the standardized precipitation evapotranspiration index: 1951–2010? *Int. J. Climatol.* 34, 545–558. doi: 10.1002/joc.3701
- Zhang, J., Huang, Y., Chen, H., Gong, J., Qi, Y., and Yang, F. (2015). Effects of grassland management on the community structure, aboveground biomass and stability of a temperate steppe in Inner Mongolia. *China. J. Arid Land Res.* 422–433. doi: 10.1007/s40333-016-0002-2
- Zhang, J., Mu, Q., and Huang, J. (2016). Assessing the remotely sensed drought severity index for agricultural drought monitoring and impact analysis in North China. *Ecol. Indic.* 63, 296–309. doi: 10.1016/j.ecolind.2015.11.062
- Zhang, X. Q., and Yamaguchi, Y. (2014). Characterization and evaluation of MODIS-derived Drought Severity Index (DSI) for monitoring the 2009/2010 drought over southwestern China. *Nat. Hazards* 74, 2129–2145. doi: 10.1007/s11069-014-1278-1
- Zhang, Y., Yu, G., Yang, J., Wimberly, M. C., Zhang, X., Tao, J., et al. (2014). Climate-driven global changes in carbon use efficiency. *Glob. Ecol. Biogeogr.* 23, 144–155. doi: 10.1111/geb.12086
- Zhao, M., Heinsch, F. A., Nemani, R. R., and Running, S. W. (2005). Improvements of the MODIS terrestrial gross and net primary production global data set. *Remote Sens. Environ.* 95, 164–176. doi: 10.1016/j.rse.2004.12.011
- Zhao, M., and Running, S. W. (2010). Drought-induced reduction in global terrestrial net primary production from 2000 through 2009. *Science* 329, 940–943. doi: 10.1126/science.1192666
- Zhao, M., and Running, S. W. (2011). Response to comments on "Drought-induced reduction in global terrestrial net primary production from 2000 through 2009". *Science* 333, 1093–1093. doi: 10.1126/science.1199169
- Zhao, M., Running, S. W., and Nemani, R. R. (2006). Sensitivity of Moderate Resolution Imaging Spectroradiometer (MODIS) terrestrial primary production to the accuracy of meteorological reanalyses. *J. Geophys. Res.* 111:G01002. doi: 10.1029/2004JG000004
- Zhou, Q., Cheng, J., Wan, H., and Yu, J. (2009). Study on the diurnal variations of photosynthetic characteristics and water use efficiency of *Stipa bungeana* Trin. under drought stress. *Acta Agrestia Sin.* 17, 510–514.

**Conflict of Interest Statement:** The authors declare that the research was conducted in the absence of any commercial or financial relationships that could be construed as a potential conflict of interest.

Copyright © 2019 Gang, Zhang, Guo, Gao, Peng, Chen and Wen. This is an open-access article distributed under the terms of the Creative Commons Attribution License (CC BY). The use, distribution or reproduction in other forums is permitted, provided the original author(s) and the copyright owner(s) are credited and that the original publication in this journal is cited, in accordance with accepted academic practice. No use, distribution or reproduction is permitted which does not comply with these terms.